Earth and Planetary Science Letters 470 (2017) 64–72

Contents lists available at ScienceDirect

Earth and Planetary Science Letters

www.elsevier.com/locate/epsl

Sulfur in foraminiferal calcite as a potential proxy for seawater carbonate ion concentration

I. van Dijk [a,*], L.J. de Nooijer [a], W. Boer [a], G.-J. Reichart [a,b]

[a] NIOZ Royal Institute for Sea Research, Department of Ocean Systems (OCS), and Utrecht University, Postbus 59, 1790 AB Den Burg, The Netherlands
[b] Utrecht University, Faculty of Geosciences, Budapestlaan 4, 3584 CD Utrecht, The Netherlands

ARTICLE INFO

Article history:
Received 16 September 2016
Received in revised form 17 March 2017
Accepted 17 April 2017
Available online 9 May 2017
Editor: H. Stoll

Keywords:
foraminifera
sulfur
culture study
carbonate system
intra-test variability

ABSTRACT

Sulfur (S) incorporation in foraminiferal shells is hypothesized to change with carbonate ion concentration [CO_3^{2-}], due to substitution of sulfate for carbonate ions in the calcite crystal lattice. Hence S/Ca values of foraminiferal carbonate shells are expected to reflect sea water carbonate chemistry. To generate a proxy calibration linking the incorporation of S into foraminiferal calcite to carbonate chemistry, we cultured juvenile clones of the larger benthic species *Amphistegina gibbosa* and *Sorites marginalis* over a 350–1200 ppm range of pCO_2 values, corresponding to a range in [CO_3^{2-}] of 93 to 211 µmol/kg. We also investigated the potential effect of salinity on S incorporation by culturing juvenile *Amphistegina lessonii* over a large salinity gradient (25–45). Results show $S/Ca_{CALCITE}$ is not impacted by salinity, but increases with increasing pCO_2 (and thus decreasing [CO_3^{2-}] and pH), indicating S incorporation may be used as a proxy for [CO_3^{2-}]. Higher S incorporation in high-Mg species *S. marginalis* suggests a superimposed biomineralization effect on the incorporation of S. Microprobe imaging reveals co-occurring banding of Mg and S in *Amphistegina lessonii*, which is in line with a strong biological control and might explain higher S incorporation in high Mg species. Provided a species-specific calibration is available, foraminiferal S/Ca values might add a valuable new tool for reconstructing past ocean carbonate chemistry.

1. Introduction

The interaction between the atmosphere and the ocean is a crucial component of the global climate system as the ocean and atmosphere exchange e.g. heat and gases. Due to the large size of the ocean it thereby acts as a reservoir and buffer for the atmosphere on geological timescales. Since the industrial revolution in the mid-18th century, ongoing anthropogenic burning of fossil fuels has resulted in a rapid increase of atmospheric CO_2 (Feely et al., 2009). Exchange of CO_2 between ocean and atmosphere has resulted in an uptake of approximately 25% of the anthropogenic carbon emissions by oceans over the last decades (Doney et al., 2009). When CO_2 enters the ocean, a suite of chemical reactions occur that lead to a decreased carbonate saturation state and the release of protons, a process called 'ocean acidification' (OA; Gattuso and Hansson, 2011). Carbonate precipitating organisms, including pteropods and coccolithophores, might be negatively impacted by these changes (Orr et al., 2005). Past ocean acidification events could provide valuable insight in the impact of ocean acidification on a global scale (Hönisch et al., 2012), but rely on our ability to accurately reconstruct carbon chemistry of the ocean. Different parameters of the ocean inorganic carbonate system are highly dependent on each other, allowing reconstruction of all parameters (e.g. pCO_2, total alkalinity, dissolved inorganic carbon [DIC] and pH) from the reconstruction of only two parameters (Zeebe and Wolf-Gladrow, 2001). Currently proxies permit reconstruction of some of these parameters (e.g. Foster, 2008; Hönisch and Hemming, 2005), whereas others are more difficult to assess. Therefore, development of new, and improvement of existing proxies is necessary to increase the accuracy and precision of such reconstructions.

Uptake of minor and trace metals in the shells of calcareous foraminifera provide a widely used toolbox to reconstruct past ocean conditions. For example, the relation between temperature and Mg incorporation in foraminiferal carbonate is reasonably well constrained (Nürnberg et al., 1996; Toyofuku et al., 2011 and references therein) and is frequently used as a paleothermometer (e.g. Elderfield and Ganssen, 2000). In comparison to temperature reconstructions, estimates of the inorganic carbon system in the past (seawater pH, alkalinity, saturation state, etc.) are less well constrained. The boron isotopic composition of

* Corresponding author.
E-mail address: Inge.van.Dijk@nioz.nl (I. van Dijk).

http://dx.doi.org/10.1016/j.epsl.2017.04.031
0012-821X/

foraminiferal shells is used as a proxy for pH (Henehan et al., 2016; Sanyal et al., 1996), while the concentrations of trace elements, including for instance U (Keul et al., 2013), Zn (Van Dijk et al., 2017) and B (Yu and Elderfield, 2007) in calcite correlate to carbonate ion concentration ($[CO_3^{2-}]$). However, partitioning of these elements is often not controlled by a single parameter (e.g., Allen and Hönisch, 2012), which is why (new) independent proxies are still needed to accurately reconstruct past ocean chemistry.

After chloride, sulfate (SO_4^{2-}) is the most abundant anion in the ocean and over geological time scales its concentration is largely controlled by the sulfur cycle (Walker, 1986). It is hypothesized that SO_4^{2-} in seawater is the only source of sulfur (S) in biogenic carbonate (Pingitore et al., 1995) and that S/Ca values change with carbonate ion concentration (Berry, 1998). Since the molar ratio of $Ca:CO_3$ in calcite is close to 1, SO_4/CO_3 can be approximated by S/Ca, which can be determined from foraminiferal shells. Over longer times scales, sulfate concentrations in the ocean have not been stable, ranging between ~10 and 30 mM during the Phanerozoic (Demicco et al., 2005), due to the balance between pyrite and shale formation/oxidation and the release of sulfur gasses (SO_2 and H_2S) by volcanic activity (Walker, 1986). Residence time of sulfate and Ca^{2+} in the ocean is currently estimated at, respectively 13–20 Ma (Bottrell and Newton, 2006) and ~1 Ma (Broecker and Peng, 1982), which implies that on timescales longer than 1 Ma foraminiferal S/Ca likely primarily reflects changes in seawater Ca^{2+} and $[SO_4^{2-}]$ (Paris et al., 2014). On shorter time scales, however, foraminiferal S/Ca values are most likely linked to seawater carbon speciation due to substitution of SO_4^{2-} for CO_3^{2-}.

Here we present and compare foraminiferal shell S/Ca data obtained from different species of benthic foraminifera cultured over either a range of pCO_2 (350–1200 ppm CO_2) or salinity (25–45), while keeping seawater S/Ca constant. Our culture set up allows us to independently quantify the impacts of these two environmental parameters on foraminiferal S/Ca, whereas in the field, these parameters are usually coupled. Furthermore, we investigate the micro-distribution of S within foraminiferal chamber walls to assess the potential biological imprint on S incorporation.

2. Methods

2.1. pCO_2-controlled experiment

2.1.1. Foraminifera collection

Macro-algae (*Dictyota* sp.) with attached larger benthic foraminifera were hand collected in November 2015 at a depth of 2–3 m in Gallows Bay, St. Eustatius (N 17°28′31.6″, W 62°59′9.4″), Caribbean Sea. Local salinity and temperature were ~34 and ~29 °C, respectively. Macro-algae samples were transported to the laboratory at the Caribbean Netherlands Science Institute (CNSI, St. Eustatius) and placed in a 5 L aquarium filled with unfiltered and aerated seawater. Algae debris was sieved over a 600 and 90 µm mesh to dislodge larger benthic foraminifera and the resulting 90–600 µm fraction was used as a stock to select specimens. Approximately 100–200 individuals of the rotaliid *Amphistegina gibbosa* and miliolid *Sorites marginalis*, characterized by yellow cytoplasm and pseudopodial activity, were isolated for the culturing experiments. Culture experiments are performed with juvenile specimens, to ensure that all calcite is grown under the set conditions of the experiment. To obtain juveniles, groups of 10–15 adults were transferred in 20 ml Petri dishes containing sand-filtered in-situ seawater and concentrated freeze-dried algae (*Dunaliella salina*) and stored at a constant temperature of 25 °C and a 12 h/12 h day/night cycle at a light intensity of approximately 300 par. After a reproduction event, juvenile clones were allowed to grow ~2 chambers before they were transferred to the culture vessel and incubated at experimental conditions.

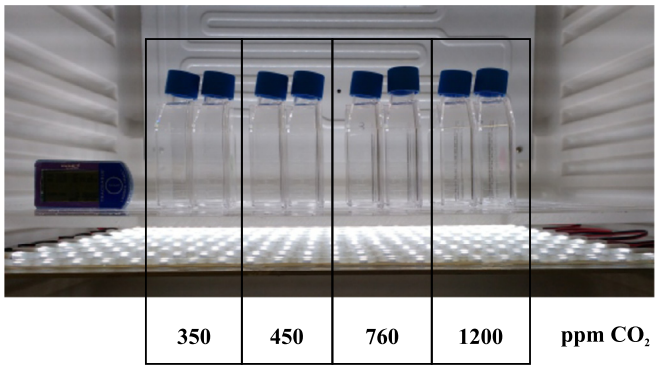

Fig. 1. Set-up of the culture experiment at 25 °C with LED shelves (300 par). Duplicate tissue bottles containing natural seawater pre-equilibrated to 350, 450, 760 or 1200 ppm CO_2 with juvenile foraminifera.

Table 1
Number of foraminifera in treatment A–D. Roman numbers indicate generation of juveniles.

Species	A	B	C	D
	350 ppm	440 ppm	760 ppm	1200 ppm
A. gibbosa	~20 (I)	~20 (I)	~20 (I)	~20 (I)
S. marginalis	~35 (I)	~35 (II)	~35 (III)	n.d.

2.1.2. Experimental set-up

Four 100 L barrels were filled with ~80 L of natural seawater (5 µm filtered). The pCO_2 in the headspace of these barrels was measured by a Li-Cor CO_2/H_2O analyzer (LI-7000), that was used to regulate addition of CO_2 and/ or CO_2-scrubbed air to keep the pCO_2 of each barrel at pre-set levels. Set-points for pCO_2 were 350 (A), 450 (B), 760 (C) and 1200 (D) ppm. This resulted in four batches of seawater with a range of pH, $[CO_3^{2-}]$ and saturation states, but with constant elemental composition, alkalinity and salinity. Salinity (34.0 ± 0.2) was measured with a salinometer (VWR CO310). Per condition, 2 L of culture water was stored bubble-free in eight 250 ml Nalgene bottles with Teflon lined Nalgene caps at 4 °C until further use. Nalgene was used because of its low gas permeability. At the start of the experiment, and for every water exchange, one of the 250 ml bottles for every of the four conditions was opened and used. This ensured that at the end of the experiment, media in the culture vessel were still in equilibrium with the pCO_2 set at the start of the experiment (see below for analytical checks).

Around eighty clones of juvenile of *A. gibbosa* and three generations (I–III) of clones of *S. marginalis* were divided in duplicates over the four pCO_2 treatments and placed in 70 ml tissue bottles with gas-tight caps (Falcon®) in a thermostat set at 25 °C (Fig. 1). This resulted in 8 tissue bottles with juvenile foraminifera (see Table 1 for specifications). Temperature within the thermostat was monitored by a temperature logger (Traceable Logger Trac, Maxi Thermal), measuring air temperature every minute. The average temperature over the whole experiment was 25 ± 0.2 °C. The shelves within the thermostat were equipped with customized LED shelfs to ensure that all foraminifera were cultured at similar light intensities. These shelves were designed to give similar amount of light (par) over a certain distance. The LED lights were controlled by a time controller and set to 30% for 12 h/12 h, which equals to 300 par (high-light condition). Light intensities were checked with an Odyssey logger (Dataflow Systems). Culture media was replaced every four days, to avoid build-up of organic waste and to obtain stable seawater element concentrations and carbon chemistry. Foraminifera were fed after every water change with 0.5 ml of freeze-dried cells of the algae *Dunaliella salina* cells, dissolved

Table 2
Carbon parameters (TA = Total Alkalinity, $n = 2$, DIC = Dissolved Inorganic Carbon, $n = 2$) with standard deviation of the culture water per treatment of the pCO_2 experiment. CO2SYS was used to calculate carbonate ion concentration and calcite saturation state and recalculate pH and atmospheric CO_2 from measured TA and DIC (VINDTA).

Treatment	Set-point	Measured			Calculated CO2SYS			
	pCO_2 (ppm)	TA (µmol/kg)	DIC VINDTA (µmol/kg)	DIC TRAACS (µmol/kg)	pCO_2 (ppm)	$[CO_3^{2-}]$ (µmol/kg)	pH (total scale)	$\Omega_{CALCITE}$
A	350	2302.8 ± 8.2	2007.5 ± 10.7	2009.1 ± 7.1	376.3	220.7	8.06	5.4
B	450	2305.2 ± 5.8	2021.3 ± 12.5	2004.0 ± 14.9	425.6	200.0	8.01	4.9
C	760	2304.4 ± 0.9	2100.8 ± 13.4	2100.2 ± 5.0	637.6	153.7	7.87	3.7
D	1200	2300.3 ± 0.7	2201.4 ± 4.1	2203.7 ± 2.6	1232.9	92.2	7.61	2.2

in seawater from the associated treatment. Foraminifera were allowed to produce new calcite for 21 days, after which they were rinsed with ultrapure water (>17 MΩ) three times, dried at 40 °C and stored in micropaleontology slides until further geochemical analysis at the NIOZ.

2.2. Salinity experiment

2.2.1. Foraminiferal collection

At Burger Zoo in Arnhem, the Netherlands, coral debris, rich in tropical foraminifera (Ernst et al., 2011), was collected from the Indo-Pacific coral reef aquarium, one of the largest coral reef aquaria in the world. Sediment was transported to the Royal Netherlands Institute of Sea Research (NIOZ), the Netherlands, and stored in aerated small aquaria at 25 °C with a day/night cycle of 12 h, mimicking the conditions in the coral reef aquarium. From this stock, living specimen of *Amphistegina*, recognized by attachment on coral debris and pseudopodial activity, were picked. These viable specimens were stored per 25 specimens in 70 ml Petri dishes with 0.2 µm North Atlantic surface seawater and addition of 1 ml/L trace metal K mix (Guillard and Ryther, 1962). After reproduction (about 2/3 of the specimens reproduced), ~2–3 chambered juveniles were incubated in the experimental conditions.

2.2.2. Experimental set-up

Five batches of 10 L of culture media with salinity increasing from 25 to 45 were obtained by diluting high-saline seawater (0.2 µm filtered North Atlantic seawater subboiled at 45 °C for 48 h to a salinity of ~50) with ultrapure water. Culture media were stored in Nalgene containers and kept in the dark at 10 °C until further use.

Juvenile specimen (2–10) were divided over Petri dishes with approximately 20 ml culture medium and placed in a thermostat set at 25 °C with a day/night cycle of 12/12 h, identical to the one depicted in Fig. 1. The culture media in the Petri dishes were replaced once a week, after which specimens were fed with approximately 1 ml of feeding solution. These feeding solutions were obtained by diluting freeze-dried *Dunaliella salina* in the appropriated culture medium of each salinity, to avoid altering the salinity of the culture media during feeding events. After 6–8 weeks, specimens were harvested and transferred to microvials for the cleaning procedure.

2.3. Analytical methods

2.3.1. Seawater carbon parameters

At the start and termination of the pCO_2-controlled experiment, 125 ml culture seawater samples of the different experimental conditions were collected to analyze the DIC and total alkalinity (TA) on a Versatile INstrument for the Determination of Titration Alkalinity (VINDTA), which was installed at the CNSI for the duration of the experiments. In addition, smaller subsamples of the culture water of all treatments were collected every four days in headspace-free vials containing a saturated $HgCl_2$ solution (10 µl $HgCl_2$/10 ml sample) and transported to the Royal NIOZ in order to re-analyze DIC on an autoanalyzer TRAACS 800 spectrometric system (Stoll et al., 2001). Subsamples of culture media from the different treatments of the salinity experiment were measure with a pH meter (pH110, VWR) and analyzed for DIC by TRAACS. Using the DIC and TA values measured on the VINDTA in the software CO2SYS v2.1, adapted to Excel by Pierrot et al. (2006), the other carbon parameters (including $[CO_3^{2-}]$ and $\Omega_{CALCITE}$) were calculated. Using the equilibrium constants for K1 and K2 from Lueker et al. (2000) and $KHSO_4$ from Dickson (1990), allows us to reconstruct $[CO_3^{2-}]$ and $\Omega_{CALCITE}$ and compare calculated pCO_2 to the set-point of the pCO_2 controller (Table 2; pCO_2 experiment, Table 3; salinity experiment).

Table 3
Carbon parameters (DIC = Dissolved Inorganic Carbon, $n = 2$; pH, $n = 4$) with standard deviation of the culture water per treatment of the *salinity* experiment. CO2SYS was used to calculate carbonate ion concentration and total alkalinity (TA).

Treatment (salinity)	Measured		Calculated CO2SYS	
	DIC (µmol/kg)	pH	TA (µmol/kg)	$[CO_3^{2-}]$ (µmol/kg)
25	1087.3 ± 2.6	8.32 ± 0.03	1352.5	164.3
30	1305.3 ± 8.1	8.28 ± 0.02	628.3	204.5
35	1512.0 ± 3.7	8.27 ± 0.02	1911.3	257.4
40	1734.4 ± 6.1	8.12 ± 0.01	2103.5	241.5
45	1947.4 ± 7.3	8.10 ± 0.02	2373.5	283.1

2.3.2. Seawater analysis using SF-ICP-MS

For the pCO_2 controlled experiment, duplicate culture water subsamples were collected in 50 ml LDPE Nalgene bottles at the start and end of the experiment and during replacement of the culture media, and immediately frozen at −80 °C. After transportation to the Royal NIOZ, the melted samples were acidified with concentrated quartz distilled HCl to pH ~1.8. For the salinity experiment, stock solutions were sampled in 50 ml LDPE Nalgene bottles at the NIOZ.

Seawater composition (^{43}Ca, ^{44}Ca, ^{24}Mg, ^{25}Mg, ^{32}S, ^{34}S, ^{87}Sr, ^{88}Sr) of all samples, as well as the seawater standard IAPSO, was analyzed on an Element-2 (ThermoFisher Scientific) magnetic sector field inductively coupled plasma mass spectrometer (SF-ICP-MS) run in medium resolution mode. Analytical precision (relative standard deviation) of the isotopes we used to calculate seawater element to calcium ratios were 3% for ^{43}Ca, ^{32}S and ^{34}S. We obtained average seawater values of 2.57 ± 0.09 mol/mol for S/Ca for the different treatments of the pCO_2 controlled experiment. For the salinity experiment, average S/Ca is 2.90 ± 0.12 mol/mol, when [S] of the culture water ranges from 22.9 mM to 33.09 mM over a salinity range of 25–45.

2.3.3. Elemental concentrations in foraminiferal calcite

2.3.3.1. Cleaning methods Specimens of *Amphistegina lessonii*, cultured over a salinity range of 25–45, were previously measured by laser ablation for another study. The specimens were transferred from the laser ablation stubs to 0.5 ml acid-cleaned TreffLab PCR-tubes. A few specimens were set apart for electron micro-

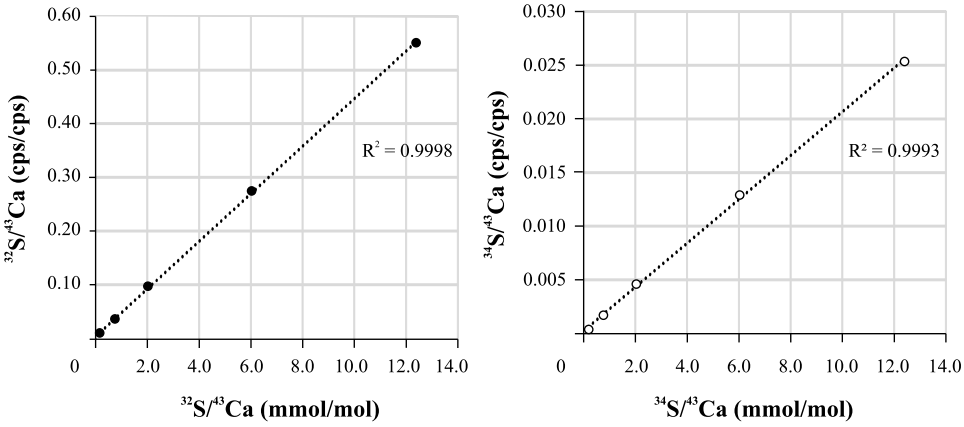

Fig. 2. Ratio calibration lines of $^{32}S/^{43}Ca$ and $^{34}S/^{43}Ca$ with R^2 value, based on the method developed by De Villiers et al. (2002).

probe analysis. Since these foraminifera had been fixed on laser ablation stub with double sided tape, we performed an additional cleaning step for only these samples to remove any traces of tape which was used to fix these specimen on the laser ablation stub. First, ultrapure water (>18.2 MΩ) was added and all vials were transferred to an ultrasonic bath (ELMA) for 1 min using moderate sound settings to keep tests intact (80 kHz, 50% power, degas function). After removal of the supernatant, this step was repeated twice. To all vials, 250 µl of suprapure methanol (Aristar) was added and again transferred to the ultrasonic bath for 1 min (same settings), after which the solvent was removed and this cleaning step repeated. In order to remove all methanol, the foraminifera were rinsed three times with ultrapure water and after the last rinse, all water was removed.

Both foraminifera from the inorganic carbon chemistry manipulation experiment (*A. gibbosa* and *S. marginalis*), as well as the above mentioned specimens from the salinity experiment (*A. lessonii*) were transferred to another set of acid-cleaned 0.5 ml PCR-tubes (TreffLab). We followed an adapted version of the protocol by Barker et al. (2003). To each vial, 250 µl of fresh prepared 1% H_2O_2 (buffered with 0.5 M NH_4OH) was added to remove organic matter. The vials were heated for 10 min in a water bath at 95 °C, and placed in an ultrasonic bath for 30 s after which the oxidizing reagent was removed. These steps (organic removal procedure) were repeated twice. Foraminiferal samples were subsequently rinsed five times with ultrapure water, dried in a laminar flow cabinet and set apart for analysis on the SF-ICP-MS.

2.3.3.2. Foraminiferal S/Ca solution analysis using SF-ICP-MS Grouped foraminifera from the pCO_2 controlled experiment (2.2.1) and from the salinity experiment (2.2.2) were transferred to 0.5 ml acid-cleaned vials and placed in a laminar flow cabin to dry. The lowest possible molarity of HNO_3 was chosen for sample dilution to decrease the S blank values. To every vial, 150 µl of ultrapure 0.05 M HNO_3 (PlasmaPURE) was added to dissolve all foraminiferal calcite. To ensure proper dissolution, vials were placed in an ultrasonic bath for 15 min (37 kHz, 100% power). Dissolution was visually checked. To determine the [Ca] in the dissolved foraminiferal calcite solutions, a five second pre-scan for ^{43}Ca in medium resolution on chromatography mode with a low flow (110 µL/min, self-aspiration) was performed on the SF-ICP-MS. Accordingly to these results, samples were diluted to obtain 100 ppm Ca. We used 5 times higher concentrations than our standard method (20 ppm Ca) to increase the S-signal of our samples and thus to increase the signal/noise ratio. These final solutions were measured again for ~120 s per sample. Masses ^{32}S, ^{34}S and ^{43}Ca were analyzed in medium resolution to separate $^{16}O^{16}O$ from the ^{32}S peaks, and $^{18}O^{16}O$ from the ^{34}S peaks. Due to low solution volumes (<500 µl) we only measured in medium resolution, and solely ^{32}S, ^{34}S and ^{43}Ca to increase precision of S/Ca. In addition to the foraminiferal samples we measured the standards NIST915a (99.97% $CaCO_3$), NFHS-1 (NIOZ Foraminifera House Standard; for details see Mezger et al., 2016) and JCp-1 (coral, Porites sp.; Okai et al., 2002) to monitor drift and the quality of the analyses. To determine foraminiferal S/Ca (mmol/mol), we used a ratio calibration method (Fig. 2; De Villiers et al., 2002). The accuracy of $^{32}S/Ca$ and $^{34}S/Ca$ based on the certified standard of JCp-1 (1900 ppm S and 53.5% CaO; Okai et al., 2002) was 102 and 105% respectively. Of the two sulfur isotopes ^{32}S is more abundant, leading to a higher signal to noise ratio and better counting statistics probably resulting in this higher accuracy. Therefore, the S/Ca presented are based on the $^{32}S/Ca$ results.

2.3.3.3. Microprobe analysis To determine the distribution of Ca, S, Mg and Sr within foraminiferal chamber walls, we analyzed cross-sections of chambers of embedded foraminifera on a field emission electron probe micro analyzer (JEOL JXA-8530F). We chose to measure *A. lessonii* from the salinity experiment, since these foraminifera grew to adult size and precipitated all their calcite under controlled conditions. First, post-ablated foraminifera were fixed in a Petri dish with double sided tape. Aluminum rings were placed in a way that one foraminifer was centered per ring. The foraminifera were placed in a house-made vacuum chamber coupled to a peristaltic pump. The rings were filled under vacuum with 2020 Araldite® resin (Huntsman International LLC) using an injector needle. After filling, the rings with resin were placed in an oven set at 45 °C for 5 days, to harden the resin and degas the sample. The embedded foraminifera were then polished with increasingly finer grained sanding paper until a cross-section of the foraminifera was visible. After a final polishing step (0.3 µm grains) foraminifera were carbon-coated and secured in the microprobe sample holder. After selection of target areas, several small high resolution maps (130 × 130 pixels, 52.9 × 52.9 µm) were analyzes at 7.0 kV using a spot diameter of 0.4072 µm and a step size of 0.4072 µm. in beam scan mode for different elements (Ca, Mg, S, Sr and Na) with a dwell time of 350 ms. The resulting concentration (level) maps were converted to qualitative Mg/Ca and S/Ca maps in MatLab by dividing the matrices. Pores and resin were avoided by excluding areas where Ca levels were <200 counts (Ca level in foraminiferal carbonate was always higher than 300 counts in our samples). For two maps we created Mg and S profiles by selecting rectangular areas (50 × 100 pixels), perpendicular to the chamber wall. The smoothed average intensities were plotted together with the organic linings (obtained from SEM photographs)

Table 4
Overview of $S/Ca_{CALCITE}$ (AVG = average; SD = standard deviation, SE = standard error) and partitioning coefficient D_S (in bold) of intermediate-Mg foraminifer *Amphistegina gibbosa* and high-Mg foraminifer *Sorites marginalis* cultured at different pCO_2 conditions.

Culture conditions		*A. gibbosa*			*S. marginalis*		
pCO_2 (ppm)	[S]/[CO_3^{2-}] (mM/µmol/kg)	AVG	SD	$D_S \times 10^{-3}$	AVG	SD	$D_S \times 10^{-3}$
350	0.12	0.95	0.03	**0.37**	8.95	0.09	**3.48**
450	0.14	1.02	0.01	**0.40**	9.60	0.10	**3.73**
760	0.18	1.10	0.03	**0.43**	10.40	0.10	**4.05**
1200	0.29	1.30	0.01	**0.51**	n.m.	n.m.	**n.m.**

Table 5
Overview of $S/Ca_{CALCITE}$ (AVG = average; SD = standard deviation, SE = standard error) and partitioning coefficient D_S (in bold) of *Amphistegina lessonii* at variable salinities, but constant [S]/[CO_3^{2-}].

Culture conditions		*A. lessonii*		
Salinity	[S]/[CO_3^{2-}] (mM/µmol/kg)	AVG	SD	$D_S \times 10^{-3}$
25	0.14	1.32	0.01	**0.46**
30	0.12	1.27	0.01	**0.44**
35	0.12	1.34	0.01	**0.46**
40	0.15	n.m.	n.m	**n.m.**
45	0.13	1.35	0.01	**0.47**

to compare the spatial relation between S and Mg bands with organic linings.

3. Results

3.1. Calcitic element concentrations

$S/Ca_{CALCITE}$ for the pCO_2 experiment (*A. gibbosa*) ranged from 0.95 to 1.30 mmol/mol (Table 4). For the salinity experiment (*A. lessonii*), we obtained average values of 1.32 for $S/Ca_{CALCITE}$ (Table 5). For *A. gibbosa*, $S/Ca_{CALCITE}$ and pCO_2 (calculated from our DIC and TA values; Table 2) are significantly ($p < 0.0010$) positively correlated (Fig. 3). No significant correlation is observed between $S/Ca_{CALCITE}$ and salinity. For *S. marginalis*, $S/Ca_{CALCITE}$ ranged from 8.95 to 10.4 mmol/mol, when pCO_2 was manipulated from 350 to 760 ppm. The average $S/Ca_{CALCITE}$ is 9.5 times higher for *S. marginalis* compared to *A. gibbosa* over the same pCO_2 range. When plotting $S/Ca_{CALCITE}$ of *A. gibbosa* and *S. marginalis* cultured in the pCO_2-controlled experiments, we observe a negative linear correlation of S/Ca with [CO_3^{2-}] for both species, albeit with an appreciable offset (Fig. 4).

3.2. Micro-distribution of S/Ca

To investigate micro-distribution of Mg, S and Sr within a foraminiferal chamber wall we analyzed two areas in a cross-section of *A. lessonii*, cultured at salinity of 25 (Fig. 5). Magnesium levels were in general ~15 times higher than S levels, and maxima occurred every ~5–7 µm (profile 1) or ~2–5 µm (profile 2). Analyzing two profiles in the target areas also revealed banding of S in the chamber wall, which on the scale studied coincides with bands high in Mg (Fig. 6). In profile 1, we observed four Mg and S bands with five organic linings. We observed seven to eight Mg and S bands and organic linings in profile 2. Comparing the position of high S and Mg bands shows that they mostly occur at or close to the organic linings, although they do not systematically overlap, as also observed for the POS by Paris et al. (2014). Both S and Mg bands show similar decreasing trends in intensity from the inner (higher ratios) to the outer (lower ratios) surface of the foraminiferal chamber wall.

4. Discussion

4.1. Sulfur in foraminifera carbonate

In biogenic carbonate, sulfur is present as SO_4^{2-} that substituted carbonate ions during calcium carbonate precipitation (Pingitore et al., 1995; Staudt et al., 1994). Besides the sulfate ions bound in the crystal lattice, sulfur-containing components (e.g. certain amino acids) may also be present in the organic matter within the shell wall (Robbins and Brew, 1990). Even though the foraminifer's cytoplasm is removed from the shell during the oxidation step in the cleaning protocol (2.3.3.1), it is possible that organic matter from e.g. the primary organic sheet (POS) and other organic linings remain trapped in-between laminar calcite layers. Potentially, part of

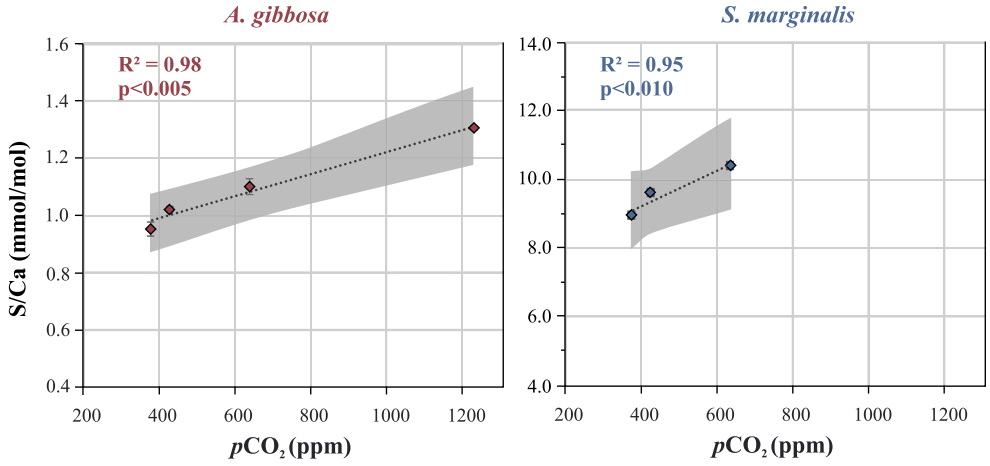

Fig. 3. Average foraminiferal S/Ca (±SD) of *A. gibbosa* (in red) and *S. marginalis* (in blue) for the four inorganic carbon treatments. Values for pCO_2 are calculated with CO2SYS (Table 2). Linear trendline with R^2, p-value and the 95% confidence interval are plotted. (For interpretation of the references to color in this figure legend, the reader is referred to the web version of this article.)

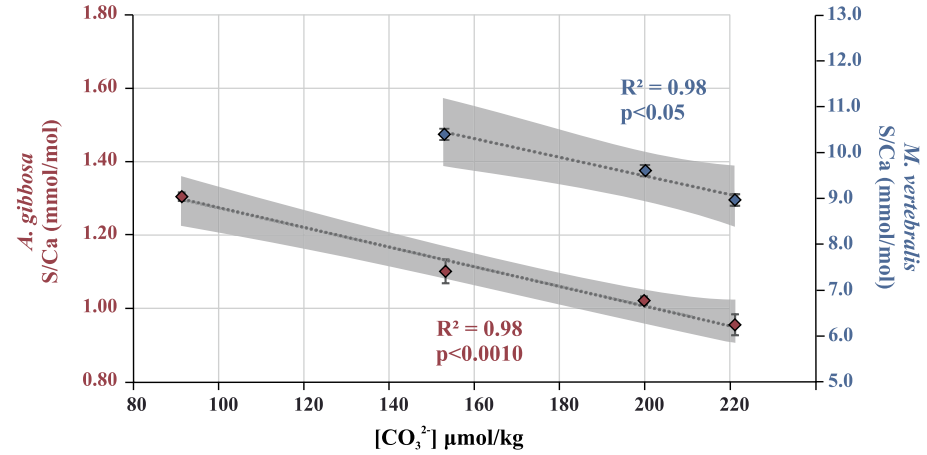

Fig. 4. Average $S/Ca_{CALCITE} \pm SD$ per treatment of *A. gibbosa* (red; $p < 0.005$) and *S. marginalis* (blue) versus $[CO_3^{2-}]$. For both species, the linear regression line (dotted lines) with R^2 and the 95% confidence interval (gray lines) are indicated. (For interpretation of the references to color in this figure legend, the reader is referred to the web version of this article.)

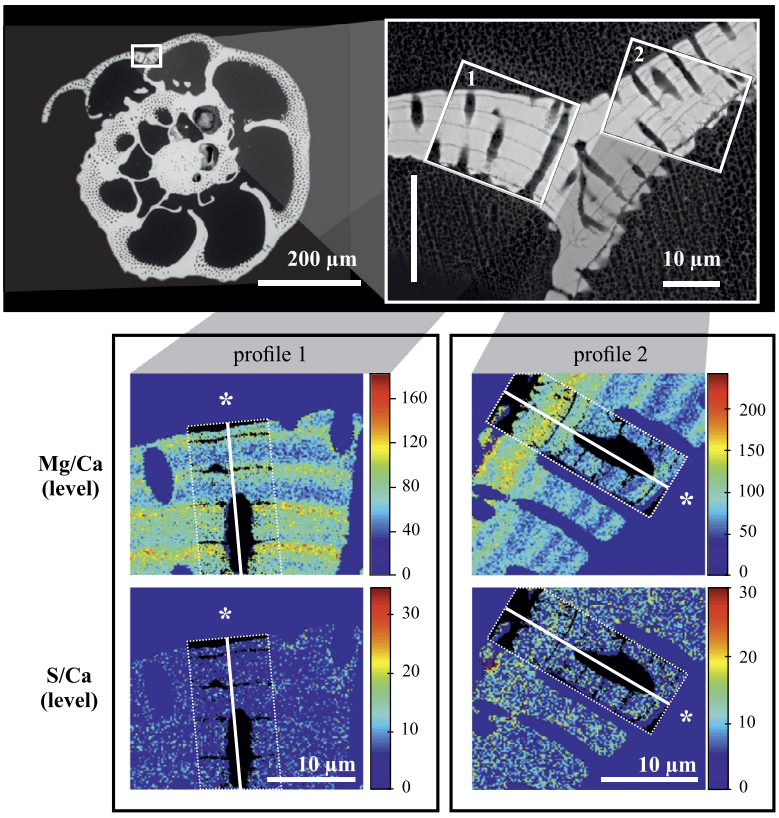

Fig. 5. Microprobe imaging of *Amphistegina lessonii*, cultured at salinity of 25. Top panels: SEM overview and close-up photograph with target areas (1 and 2). Lower panels: Microprobe areas (1 and 2) with Mg/Ca (top) and S/Ca (bottom) in counts/counts with organic sheet overlay of areas of interest (dotted layer) and profile lines (white). Asterisk indicates the outside surface of the foraminiferal shell wall.

the total S measured by SF-ICP-MS could originate from these organic components. The total amount of organic material found in the shells of *Heterostegina depressa* is 0.1–0.2 wt% of the total shell and is mainly composed of two fractions: one consisting of potentially heavily sulfated polysaccharides (glycosaminoglycans) and one with mainly proteins (Weiner and Erez, 1984). The former fraction contains approximately 16% sulfur by weight (e.g. chondroitin sulfate), whereas the protein fraction contains very little sulfur (like aspartate, glutamate, serine). The amount of sulfur-containing amino acids in this fraction contributes less than 5% to the total amino acids, and of this 5% at most 30% in weight is sulfur (Robbins and Brew, 1990). The relative contributions of the protein and polysaccharide fractions within foraminiferal shells differs between species and is poorly quantified (Ní Fhlaithearta et al., 2013). However, assuming that both fractions contribute equally to the total organic weight, 0.009–0.018 wt% of the shell would be organic sulfur, which is in line with pyrolysis GC-MS analyses of isolated organic linings from foraminiferal shells (Ní Fhlaithearta et al., 2013). Still, since S content in our foraminifera was between ~2000 and 3000 ppm, potentially up to 5% of our S signal could be derived from organic-bound S. This value is higher than the 1.1% organic sulfur calculated by Paris et al. (2014), since the contribution from sulfated polysaccharides was not taken into account in their calculations. Since the peaks in the sulfur intensity do not

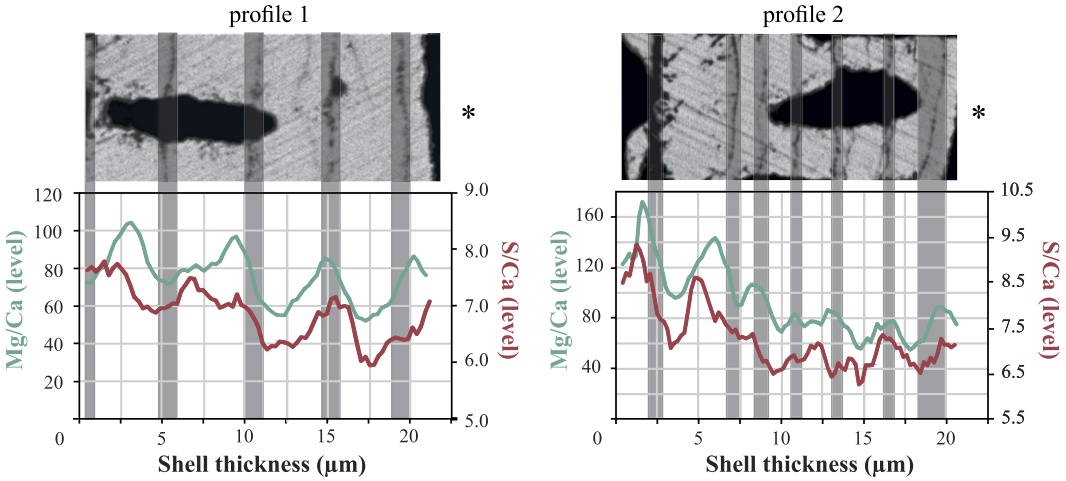

Fig. 6. SEM photographs of profile areas 1 and 2 (Fig. 4) with average Mg (green) and S (red) levels (counts/counts) across profile area 1 (left) and 2 (right). Dark gray panels are areas associated with organic linings, identified on the SEM pictures (Fig. 4). Asterisk indicates the outside of the foraminifera. (For interpretation of the references to color in this figure legend, the reader is referred to the web version of this article.)

fully correspond to the position of the organic linings (our study; Paris et al., 2014), and the lack of sulfurized polysaccharides in isolated foraminiferal organic linings (Ní Fhlaithearta et al., 2013) also in our case the contribution of organic-bound S was most likely effectively removed by the oxidative step and considerably smaller than 5%.

4.2. Controls on S/Ca in foraminiferal calcite

Sulfur incorporation varies with pCO_2 in both the intermediate-Mg foraminifer *A. gibbosa* ($p < 0.005$) and the high-Mg foraminifer *S. marginalis* ($p < 0.010$; Fig. 4). When assuming a linear relation between S incorporation and $[CO_3^{2-}]$, $S/Ca_{CALCITE}$ decreases with 20% per 100 µmol/kg $[CO_3^{2-}]$ increase for *A. gibbosa*, and 18% for *S. marginalis*, suggesting S incorporation in both species is governed by the same underlying process. Assuming all S incorporated in foraminiferal calcite is the result of lattice substitution of SO_4 for CO_3, we expect foraminiferal S/Ca to linearly decrease with increasing $[CO_3^{2-}]$, since SO_4 would be outcompeted by CO_3. However, based on the experiment as such, also several other parameters of the carbonate system could be responsible for the observed trend in S/Ca as in the pCO_2 experiment several parameters changed in concert. Still, as sulfate speciation in seawater does not change over the pH interval studied here, S/Ca most likely varies directly as a function of SO_4/CO_3.

We observed no systematic impact of salinity on $S/Ca_{CALCITE}$ (Table 5). In the salinity experiments also $[CO_3^{2-}]$ changed, as alkalinity and salinity correlated linearly. Still, seawater $[SO_4^{2-}]$ had no detectable impact on S/Ca when seawater [S] was varied between 22.9 mM to 33.09 mM in the experiment with varying salinity. Because the S/CO_3 of the media was constant, also foraminiferal S/Ca remained relatively constant despite varying $[CO_3^{2-}]$. In contrast, in the pCO_2 controlled experiment (Fig. 3) S/Ca increased with increasing seawater S/CO_3 and hence decreasing $[CO_3^{2-}]$ and pH (Table 4). This suggests that $S/Ca_{CALCITE}$ may be a useful tool to reconstruct changes in seawater $[CO_3^{2-}]$ over timescales up to ~1 Ma (residence time of Ca^{2+}; Broecker and Peng, 1982), or when seawater $[SO_4^{2-}]$ is known, also over longer time scales. However, superimposed on the impact of $[CO_3^{2-}]$ on S incorporation, biomineralization also impacts foraminiferal S/Ca, and species-specific differences therein are likely responsible for the observed offset in S/Ca between the hyaline *A. gibbosa* and miliolid *S. marginalis*. To increase the robustness of this potential proxy, future experiments have to include adult specimens, to assess possible ontogenetic effects on S incorporation. Also the observed banding (Figs. 5 and 6) and co-occurrence of S/Ca-banding with Mg/Ca banding suggests a biomineralization related control on S incorporation.

4.3. Banding in foraminiferal carbonate

Certain elements have a heterogeneous distribution in foraminiferal chamber walls, often expressed as banding of these elements. Banding has been reported for a variety of species, including large benthic foraminifera (Evans and Müller, 2013), planktonic species with symbionts (e.g. Kunioka et al., 2006; Paris et al., 2014) and without symbionts (Sadekov et al., 2005). Our results show that banding of Mg and S is present in the larger benthic foraminifer *A. lessonii* and that bands with elevated concentrations of Mg and S co-occur within the chamber wall, close to organic layers (Fig. 6). This implies that phases of high Mg and high S formed simultaneously during calcification and hence potentially that their incorporation may be mechanistically linked.

The bilamellar calcification model suggests that chamber formation in hyaline foraminifera starts with the formation of the primary organic sheet (POS), after which the first stages of calcification commence by precipitation of carbonate on either side of the POS (Erez, 2003 and references therein). This model combined with our observations suggests that the initial carbonate is enriched in several elements, with the bands high in Mg and S close to the POS (Fig. 6). Banding observed in the outer part of the chamber wall are linked to organic sheets that are formed during calcification of successive chambers (known as outer organic layers or OOL), enveloping the rest of the test. The banding in S and Mg (Fig. 6) and their relation with organic layers suggests that the processes responsible for delivery of ions to the site of calcification (SOC) are not constant over time. This may be explained by the two processes that transport ions from the surrounding seawater to the SOC (i.e. passive supply and active transmembrane transport; Nehrke et al., 2013) of which the relative contribution changes as the calcite wall grows. While ongoing chamber wall formation is promoted by active Ca^{2+} pumping into the SOC by transmembrane transport, internal pH and hence carbonate speciation also changes due to the associated proton removal (De Nooijer et al., 2009). Hence, both Mg/Ca and SO_4/CO_3 decrease at the SOC with ongoing calcification, albeit not necessarily at the same rate, as observed in the cross sections of these elements incorporated. The large role of biomineralization at the same time also explains the overall differences in elemental composition observed in high- and low-Mg producing foraminifera.

Element incorporation in the calcite of the miliolid *S. marginalis* however, may not be caused by the mechanisms proposed in existing calcification models (De Nooijer et al., 2014 and references therein), since miliolid foraminifera produce their calcite in a fundamentally different way as hyaline foraminifera do. The overall high Mg/Ca ratios in miliolid foraminifera (e.g. Bentov and Erez, 2006) are comparable to (or even somewhat higher than) what is expected based on inorganic partition coefficients (Mucci, 1987). In the terminology of the passive transport model of Nehrke et al. (2013) this corresponds to a very large contribution of the seawater vacuoles. Hence, major, minor and trace element composition in the seawater-derived vacuoles is only slightly modified and the calcite needles precipitate in the presence of relatively high $[Mg^{2+}]$ and high SO_4/CO_3 values.

4.4. Internal pH

Even though hyaline and miliolid species have a fundamentally different way of precipitating their shells, it has been shown that both groups increase their internal pH to promote precipitation of calcite (De Nooijer et al., 2009), while the pH in the foraminiferal microenvironment decreases (Glas et al., 2012; Toyofuku et al., 2017). Increasing the pH at the site of calcification would shift the most dominant form of DIC from HCO_3^- to CO_3^{2-} and hence increase the saturation state in the SOC. However, it is not known whether foraminifera increase their internal pH up to a set value (e.g. pH = 9) or that they elevate their internal pH by a fixed value compared to ambient pH (Ries, 2011). Which of these two alternatives characterizes foraminiferal proton pumping, however, is important for the incorporation of ions other than Ca^{2+} and carbonate.

When internal pH increases to a certain set value, incorporation of elements of which the chemical speciation depends strongly on pH is not expected to vary as a function of ambient pH/saturation state/$[CO_3^{2-}]$. Instead, incorporation of these elements would always be determined by the same, internal pH at the site of calcification. Since e.g. foraminiferal Zn/Ca and U/Ca changes with $[CO_3^{2-}]$ (Keul et al., 2013), and the boron isotopic signature of foraminiferal calcite changes as a function of pH (Sanyal et al., 1996), it is more likely that foraminifera increase their internal pH by a set difference compared to the external seawater pH. This implies that a 0.4 pH unit change in seawater pH (lowest–highest of our pCO_2 treatments), also results in a 0.4 pH unit change in the internal pH. Assuming a 1 unit offset during calcification, this would translate to an increase in pH at the SOC between the experiments from 8.6 to 9.0. Using CO2SYS, we can calculate the associated increase of the internal $[CO_3^{2-}]$ is an increase of ∼37%, which matches well with the decrease of 36.8% $S/Ca_{CALCITE}$ observed for *A. gibbosa* with a pH change of 0.4 units. Therefore, the observed decrease in S/Ca hints to maintenance of a high internal pH with a fixed difference compared to the surrounding seawater pH.

5. Conclusions

Sulfur incorporation in foraminiferal calcite does not significantly change over a large salinity gradient (25–45), but seems to change linearly with inorganic carbon speciation. We propose that seawater $[CO_3^{2-}]$ is the main parameter affecting S/Ca in foraminiferal calcite, due to lattice substitution of sulfate for carbonate ions. Microprobe imaging reveals S banding within the chamber wall, which more or less co-occurs with Mg banding. The miliolid foraminifer *Sorites marginalis* incorporates more S than hyaline *Amphistegina gibbosa*, hinting at an underlying biomineralization signal. Foraminiferal S/Ca provides the potential to reconstruct past seawater carbonate chemistry when taking into account species-specific differences in incorporated sulfur.

Acknowledgements

This research is funded by the NIOZ – Royal Netherlands Institute for Sea Research and the Darwin Centre for Biogeosciences project 3020: “Double Trouble: Consequences of Ocean Acidification – Past, Present and Future – Evolutionary changes in calcification mechanisms” and the program of the Netherlands Earth System Science Center (NESSC). We would like to thank the editor and two anonymous reviewers for the constructive comments. Great thanks to the Johan Stapel of the CNSI, for hosting the 2015 foraminifera culture expedition on St. Eustatius, as well as all participants: Jelle Bijma and Gernot Nehrke from the AWI, Brett Metcalfe (VU), Esmee Geerken (NIOZ), Alice Webb (NIOZ) and Didier de Bakker (NIOZ/IMARES). Bob Koster and Steven van Heuven are thanked for designing and constructing the controlled pCO_2 setup used in this study (NWO grants 858.14.021 and 858.14.022). Esmee Geerken is thanked for support with the salinity culture experiment at the NIOZ and microprobe image processing. Furthermore, we would like to thank Kirsten Kooijman for supplying *Dunaliella salina*, Patrick Laan and Karel Bakker for seawater analysis, Leonard Bik and Michiel Kienhuis for their help with polishing, Sergei Matveev and Tilly Bouten for providing technical support with the microprobe at University of Utrecht.

References

Allen, K.A., Hönisch, B., 2012. The planktic foraminiferal B/Ca proxy for seawater carbonate chemistry: a critical evaluation. Earth Planet. Sci. Lett. 345–348, 203–211.
Barker, S., Higgins, J.A., Elderfield, H., 2003. The future of the carbon cycle: review, calcification response, ballast and feedback on atmospheric CO_2. Philos. Trans. R. Soc. A, Math. Phys. Eng. Sci. 361, 1977–1998. Discussion 1998–1979.
Bentov, S., Erez, J., 2006. Impact of biomineralization processes on the Mg content of foraminiferal shells: a biological perspective. Geochem. Geophys. Geosyst. 7. http://dx.doi.org/10.1029/2005GC000960.
Berry, J.N., 1998. Sulfate in Foraminiferal Calcium Carbonate: Investigating a Potential Proxy for Sea Water Carbonate Ion Concentration. Massachusetts Institute of Technology, Cambridge, p. 88.
Bottrell, S.H., Newton, R.J., 2006. Reconstruction of changes in global sulfur cycling from marine sulfate isotopes. Earth-Sci. Rev. 75, 59–83.
Broecker, W.S., Peng, T.-H., 1982. Tracers in the Sea. Lamont–Doherty Geological Observatory, Columbia University.
De Nooijer, L.J., Spero, H.J., Erez, J., Bijma, J., Reichart, G.J., 2014. Biomineralization in perforate foraminifera. Earth-Sci. Rev. 135, 48–58.
De Nooijer, L.J., Toyofuku, T., Kitazato, H., 2009. Foraminifera promote calcification by elevating their intracellular pH. Proc. Natl. Acad. Sci. USA 106, 15374–15378.
De Villiers, S., Greaves, M., Elderfield, H., 2002. An intensity ratio calibration method for the accurate determination of Mg/Ca and Sr/Ca of marine carbonates by ICP-AES. Geochem. Geophys. Geosyst. 3. http://dx.doi.org/10.1029/2001GC000169.
Demicco, R.V., Lowenstein, T.K., Hardie, L.A., Spencer, R.J., 2005. Model of seawater composition for the Phanerozoic. Geology 33, 877.
Dickson, A.G., 1990. Thermodynamics of the dissociation of boric acid in synthetic seawater from 273.15 to 318.15 K. Deep Sea Res. Part A, Oceanogr. Res. Pap. 37, 755–766.
Doney, S.C., Fabry, V.J., Feely, R.A., Kleypas, J.A., 2009. Ocean acidification: the other CO_2 problem. Annu. Rev. Mar. Sci. 1, 169–192.
Elderfield, H., Ganssen, G., 2000. Past temperature and $\delta^{18}O$ of surface ocean waters inferred from foraminiferal Mg/Ca ratios. Nature 405, 442–445.
Erez, J., 2003. The source of ions for biomineralization in foraminifera and their implications for paleoceanographic proxies. Rev. Mineral. Geochem. 54, 115–149.
Ernst, S., Janse, M., Renema, W., Kouwenhoven, T., Goudeau, M.-L., Reichart, G.-J., 2011. Benthic foraminifera in a large Indo-Pacific coral reef aquarium. J. Foraminiferal Res. 41, 101–113.
Evans, D., Müller, W., 2013. LA-ICP-MS elemental imaging of complex discontinuous carbonates: an example using large benthic foraminifera. J. Anal. At. Spectrom. 28, 1039–1044.
Feely, R.A., Doney, S.C., Cooley, S.R., 2009. Ocean acidification: present conditions and future changes in a high-CO_2 world. Oceanography 22, 36–47.
Foster, G.L., 2008. Seawater pH, pCO2 and [CO2–3] variations in the Caribbean Sea over the last 130 kyr: a boron isotope and B/Ca study of planktic foraminifera. Earth Planet. Sci. Lett. 271, 254–266.
Gattuso, J.-P., Hansson, L., 2011. Ocean Acidification. OUP, Oxford.
Glas, M.S., Langer, G., Keul, N., 2012. Calcification acidifies the microenvironment of a benthic foraminifer (*Ammonia sp.*). J. Exp. Mar. Biol. Ecol. 424–425, 53–58.
Guillard, R.R.L., Ryther, J.H., 1962. Studies of marine planktonic diatoms: I. Cyclotella nana Hustedt, and Detonula confervacea (cleve) Gran. Can. J. Microbiol. 8, 229–239.

Henehan, M.J., Foster, G.L., Bostock, H.C., Greenop, R., Marshall, B.J., Wilson, P.A., 2016. A new boron isotope-pH calibration for Orbulina universa, with implications for understanding and accounting for 'vital effects'. Earth Planet. Sci. Lett. 454, 282–292.

Hönisch, B., Hemming, N.G., 2005. Surface ocean pH response to variations in pCO_2 through two full glacial cycles. Earth Planet. Sci. Lett. 236, 305–314.

Hönisch, B., Ridgwell, A., Schmidt, D.N., Thomas, E., Gibbs, S.J., Sluijs, A., Zeebe, R., Kump, L., Martindale, R.C., Greene, S.E., Kiessling, W., Ries, J., Zachos, J.C., Royer, D.L., Barker, S., Marchitto, T.M., Moyer, R., Pelejero, C., Ziveri, P., Foster, G.L., Williams, B., 2012. The geological record of ocean acidification. Science 335, 1058–1063.

Keul, N., Langer, G., De Nooijer, L.J., Nehrke, G., Reichart, G.-J., Bijma, J., 2013. Incorporation of uranium in benthic foraminiferal calcite reflects seawater carbonate ion concentration. Geochem. Geophys. Geosyst. 14, 102–111.

Kunioka, D., Shirai, K., Takahata, N., Sano, Y., Toyofuku, T., Ujiie, Y., 2006. Microdistribution of Mg/Ca, Sr/Ca, and Ba/Ca ratios in *Pulleniatina obliquiloculata* test by using a NanoSIMS: implication for the vital effect mechanism. Geochem. Geophys. Geosyst. 7. http://dx.doi.org/10.1029/2006gc001280.

Lueker, T.J., Dickson, A.G., Keeling, C.D., 2000. Ocean pCO2 calculated from dissolved inorganic carbon, alkalinity, and equations for K1 and K2: validation based on laboratory measurements of CO2 in gas and seawater at equilibrium. Mar. Chem. 70, 105–119.

Mezger, E.M., de Nooijer, L.J., Boer, W., Brummer, G.J.A., Reichart, G.J., 2016. Salinity controls on Na incorporation in Red Sea planktonic foraminifera. Paleoceanography 31 (12), 1562–1582.

Mucci, A., 1987. Influence of temperature on the composition of magnesian calcite overgrowths precipitated from seawater. Geochim. Cosmochim. Acta 51, 1977–1984.

Nehrke, G., Keul, N., Langer, G., De Nooijer, L.J., Bijma, J., Meibom, A., 2013. A new model for biomineralization and trace-element signatures of foraminifera tests. Biogeosciences 10, 6759–6767.

Ní Fhlaithearta, S., Ernst, S.R., Nierop, K.G., de Lange, G.J., Reichart, G.-J., 2013. Molecular and isotopic composition of foraminiferal organic linings. Mar. Micropaleontol. 102, 69–78.

Nürnberg, D., Bijma, J., Hemleben, C., 1996. Assessing the reliability of magnesium in foraminiferal calcite as a proxy for water mass temperatures. Geochim. Cosmochim. Acta 60, 803–814.

Okai, T., Suzuki, A., Kawahata, H., Terashima, S., Imai, N., 2002. Preparation of a new geological survey of Japan geochemical reference material: coral JCp-1. Geostand. Newsl. 26, 95–99.

Orr, J.C., Fabry, V.J., Aumont, O., Bopp, L., Doney, S.C., Feely, R.A., Gnanadesikan, A., Gruber, N., Ishida, A., Joos, F., Key, R.M., Lindsay, K., Maier-Reimer, E., Matear, R., Monfray, P., Mouchet, A., Najjar, R.G., Plattner, G.K., Rodgers, K.B., Sabine, C.L., Sarmiento, J.L., Schlitzer, R., Slater, R.D., Totterdell, I.J., Weirig, M.F., Yamanaka, Y., Yool, A., 2005. Anthropogenic ocean acidification over the twenty-first century and its impact on calcifying organisms. Nature 437, 681–686.

Paris, G., Fehrenbacher, J.S., Sessions, A.L., Spero, H.J., Adkins, J.F., 2014. Experimental determination of carbonate-associated sulfate $\delta^{34}S$ in planktonic foraminifera shells. Geochem. Geophys. Geosyst. 15, 1452–1461.

Pierrot, D., Lewis, E., Wallace, D.W.R., 2006. MS Excel Program Developed for CO_2 System Calculations. ORNL/CDIAC-105a. Carbon Dioxide Information Analysis Center, Oak Ridge National Laboratory, U.S.

Pingitore, N.E., Meitzner, G., Love, K.M., 1995. Identification of sulfate in natural carbonates by X-ray absorption spectroscopy. Geochim. Cosmochim. Acta 59, 2477–2483.

Ries, J.B., 2011. A physicochemical framework for interpreting the biological calcification response to CO_2-induced ocean acidification. Geochim. Cosmochim. Acta 75, 4053–4064.

Robbins, L.L., Brew, K., 1990. Proteins from the organic matrix of core-top and fossil planktonic foraminifera. Geochim. Cosmochim. Acta 54, 2285–2292.

Sadekov, A.Y., Eggins, S.M., De Deckker, P., 2005. Characterization of Mg/Ca distributions in planktonic foraminifera species by electron microprobe mapping. Geochem. Geophys. Geosyst. 6. http://dx.doi.org/10.1029/2005GC000973.

Sanyal, A., Hemming, N.G., Broecker, W.S., Lea, D.W., Spero, H.J., Hanson, G.N., 1996. Oceanic pH control on the boron isotopic composition of foraminifera: evidence from culture experiments. Paleoceanography 11, 513–517.

Staudt, W.J., Reeder, R.J., Schoonen, M.A.A., 1994. Surface structural controls on compositional zoning of SO^{2-4} and SeO^{2-4} in synthetic calcite single crystals. Geochim. Cosmochim. Acta 58, 2087–2098.

Stoll, M.H.C., Bakker, K., Nobbe, G.H., Haese, R.R., 2001. Continuous-flow analysis of dissolved inorganic carbon content in seawater. Anal. Chem. 73, 4111–4116.

Toyofuku, T., Matsuo, M.Y., de Nooijer, L.J., Nagai, Y., Kawada, S., Fujita, K., Reichart, G.-J., Nomaki, H., Tsuchiya, M., Sakaguchi, H., Kitazato, H., 2017. Proton pumping accompanies calcification in foraminifera. Nat. Commun. 8. http://dx.doi.org/10.1038/ncomms14145. Article number: 14145.

Toyofuku, T., Suzuki, M., Suga, H., Sakai, S., Suzuki, A., Ishikawa, T., De Nooijer, L.J., Schiebel, R., Kawahata, H., Kitazato, H., 2011. Mg/Ca and $\delta^{18}O$ in the brackish shallow-water benthic foraminifer *Ammonia 'beccarii'*. Mar. Micropaleontol. 78, 113–120.

Van Dijk, I., De Nooijer, L.J., Wolthers, M., Reichart, G.-J., 2017. Impacts of pH and $[CO_3^{2-}]$ on the incorporation of Zn in foraminiferal calcite. Geochim. Cosmochim. Acta 197, 263–277.

Walker, J.C., 1986. Global geochemical cycles of carbon, sulfur and oxygen. Mar. Geol. 70, 159–174.

Weiner, S., Erez, J., 1984. Organic matrix of the shell of the foraminifer, *Heterostegina depressa*. J. Foraminiferal Res. 14, 206–212.

Yu, J., Elderfield, H., 2007. Benthic foraminiferal B/Ca ratios reflect deep water carbonate saturation state. Earth Planet. Sci. Lett. 258, 73–86.

Zeebe, R.E., Wolf-Gladrow, D.A., 2001. CO_2 in Seawater: Equilibrium, Kinetics, Isotopes. Gulf Professional Publishing.